J Polym Res (2017) 24: 71
DOI 10.1007/s10965-017-1232-5

ORIGINAL PAPER

Effect of varying hydrolysis time on extraction of spherical bacterial cellulose nanocrystals as a reinforcing agent for poly(vinyl alcohol) composites

Nga Tien Lam[1] · **Wipanee Saewong**[1] · **Prakit Sukyai**[1]

Received: 16 September 2016 / Accepted: 6 April 2017 / Published online: 14 April 2017

Abstract Bacterial cellulose nanocrystal (BCNC) was prepared from bacterial cellulose (BC) using acid hydrolysis for 12, 24 and 72 h. The effect of the BCNC was estimated as a means of reinforcing the poly(vinyl alcohol) (PVA) matrix in terms of mechanical and thermal properties. The effect of the hydrolysis time on BCNC extraction was evaluated by considering morphology, changes in chemical functional groups, crystallinity and thermal stability. Atomic force microscopy (AFM) images revealed the diameters of spherical cellulosic particles were in the range 16–35 nm with the smaller ones resulting from a longer hydrolysis treatment time. Fourier transform infrared (FTIR) spectroscopy showed no changes in the functional groups between BC and BCNC samples for all hydrolysis extraction times. However, X-ray diffraction (XRD) proved that the crystallinity of the BCNC increased up to 87% in comparison with the BC. The thermal stability of nanocellulose decreased over a longer hydrolysis period. Furthermore, the BCNC showed an improved effect on the PVA matrix in both tensile and thermal analysis. Therefore, BCNC obtained by acid hydrolysis for 24 h could be used as a reinforcing agent for material industries.

Keywords Spherical bacterial cellulose nanocrystals · Acid hydrolysis time · Poly(vinyl alcohol) · Reinforcement

✉ Prakit Sukyai
fagipks@ku.ac.th

[1] Biotechnology of Biopolymers and Bioactive Compounds Special Research Unit, Department of Biotechnology, Faculty of Agro-Industry, Kasetsart University, Chatuchak, Bangkok 10900, Thailand

Introduction

Cellulose is the most abundant polymer, consisting of a linear chain of D-glucose units linked by a $\beta(1 \rightarrow 4)$ glycosidic bond [1, 2]. Extraction of cellulose has been reported from wood, cotton, wheat straw and rice straw [3–6]. However, in recent years, cellulose production by *Gluconacetobacter xylinum* is known as bacterial cellulose that composed of ribbon-shaped nanofibril bundles [7, 8]. This bacterial strain produces a bacterial cellulose layer at the interface in a static culture medium. In fact, plant cellulose and BC share the same chemical structure, however, their properties are different. Plant cellulose, a lignocellulose mainly consists of cellulose, hemicellulose and lignin while BC contented cellulose only with a high purity, high crystallinity, high mechanical strength and biocompatibility [9–11]. Due to the outstanding properties of BC, it can be applied for various applications, including as a filled network for polymeric matrixes, nanocomposites, bioplastics, biomedicines and in the paper industry [8–10, 12–15].

In general, BC is commonly used in the form of nanocellulose, due to its unique properties, having high crystallinity between 54 and 88%, a range width of 5–70 nm and a length from 100 nm to several micrometers [16]. A procedure widely used for the extraction of cellulose nanocrystals (CNC) is sulfuric acid hydrolysis, which involves preferential hydrolysis of the amorphous region that can cause increased crystallinity [2]. During hydrolysis, esterification happens along the cellulose domains at OH groups, which is replaced by a sulfate group. Thus, nanocellulose become an aqueous suspension which is negatively charged and so does not coagulate [17].

It is well-documented that there are at least rod, spherical and network morphologies of CNC that can be extracted using sulfuric acid from cotton [18, 19]. The aggregation of rod-like CNCs leads to crystalline phase forms in an aqueous

suspension whereas colloidal crystallization results with spherical CNCs because of their high and similar surface areas [20]. In addition, spherical CNCs with a large interacting surface have the ability to connect to others particles, such as polymeric matrices, bioactive compounds and living cells [7]. On the other hand, BC has no portion of hemicellulose and lignin that must be eliminated, so the solid yield can be up to 89% according to the BC dry weight [21, 22]. Due to the highly networked structure of BC, the hydrolysis conditions have been varied to optimum for breaking its amorphous domains. This can result in the degradation of cellulose to shorter nanocrystals [21]. Therefore, spherical bacterial cellulose nanocrystals (BCNC) have been successfully extracted from BC using acid hydrolysis. In the previous research, the optimum time of acid hydrolysis was applied at 2, 48 and 69 h and the obtained BCNC at 48 h got the highest crystallinity percentage in comparison with others [22].

Current techniques to upgrade the mechanical properties of nanocomposites have extensively considered adding nano particles as reinforcing agents and these have been highly beneficial to the industrial sector [2, 7, 23–26]. The nanocellulose was added to reinforce for poly(styrene-co-butyl acrylate) matrix examined by Favier et al. [27] and in starch-based polymers conducted by Kvien et al. [28]. Poly(vinyl alcohol) (PVA) is a kind of the biodegradable polymers using in diverse industries due to its hydrophilic, film forming and non-toxicity [29–31] and it is used in various industrial applications such as paints, shampoos, packaging films, paper adhesives, textile and paper coatings [32].

To the best of our knowledge, there has not been any reports about investigating the use of spherical BCNCs to reinforce PVA matrix composites. Therefore, the objectives of this study were to determine the effect of varying the hydrolysis time on the characterization of spherical BCNC and the reinforcing ability of BCNC in PVA composites in terms of its thermal and mechanical properties.

Materials and methods

Preparation of BC

A sample of 100 ml of the bacterial strain *Gluconacetobacter xylinum* starter was incubated in 1000 ml of coconut juice medium composed of 5% sucrose, 0.5% ammonium sulfate and 5% acetic acid (10% *v*/v), at 30 °C for 5–7 days. A BC layer was produced on the top of the surface medium. The BC was purified by boiling in distilled water for 15 min, neutralizing in an aqueous solution of 1% (*v*/v) NaOH at room temperature for 24 h and rinsed with distilled water up to pH of 7. Then, the BC was compressed to remove excess water and ground into powder.

Extraction of BCNC

The BC powder was treated with 60% (*w*/w) sulfuric acid with a cellulose-to-acid ratio of 1:20 g/ml under stirring at 45 °C with different hydrolysis times of 12, 24 and 72 h which were recorded as BCNC-12, BCNC-24 and BCNC-72, respectively. Distilled water was added to stop the reaction (approximately 4 °C) in the volume of sulfuric acid used and then centrifuged at 13000 rpm and 4 °C for 15 min. The centrifugation step involved at least two or three washings to remove the residual acid. The obtained BCNC was neutralized using dialysis, until the pH of the samples was neutral (pH 6–7). Then the samples were sonicated for 30 min and stored in the refrigerator.

Preparation of PVA/BCNC

Poly(vinyl alcohol) (PVA) (M_w = 77,000–82,000) was dissolved at 80 °C for 3 h. BCNC-24 suspension was added at 1, 3 and 5%wt. The mixture (PVA/BCNC) was further stirred for another 3 h and sonicated for 30 min before being cast onto glass plates. The films were dried at 50 °C for 12 h. The obtained films were kept in a desiccator for further analysis.

Characterization

Morphology analysis of BCNC

Atomic force microscopy (AFM) was used to characterize the morphology of the dimensional image of nanocellulose obtained from the acid hydrolyzed samples. Measurements were performed in tapping mode using an Asylum model MFP-3D AFM (Bio, USA) at ambient temperature. In the sample preparation, a drop of diluted aqueous suspension of colloid was dispersed on the surface of an optical glass substrate and allowed to dry at ambient temperature and analyzed subsequently.

Fourier transform infrared (FTIR) spectrometer analysis of BCNC

Infrared spectra of the samples were recorded using an FTIR spectrometer (Bruker Tensor 27 spectrometer, USA) at room temperature. The sample fractions were dried in an oven at 60 °C for 12 h, mixed with KBr and pressed into pellets. The samples were analyzed over the range 500–4000 cm^{-1}.

X-ray diffraction (XRD)

XRD measurements were acquired using an X-ray diffractometer (Philips Analytical X'Pert, the Netherlands) using Cu-Kα radiation (1.5418 nm). The angle was scanned in the range

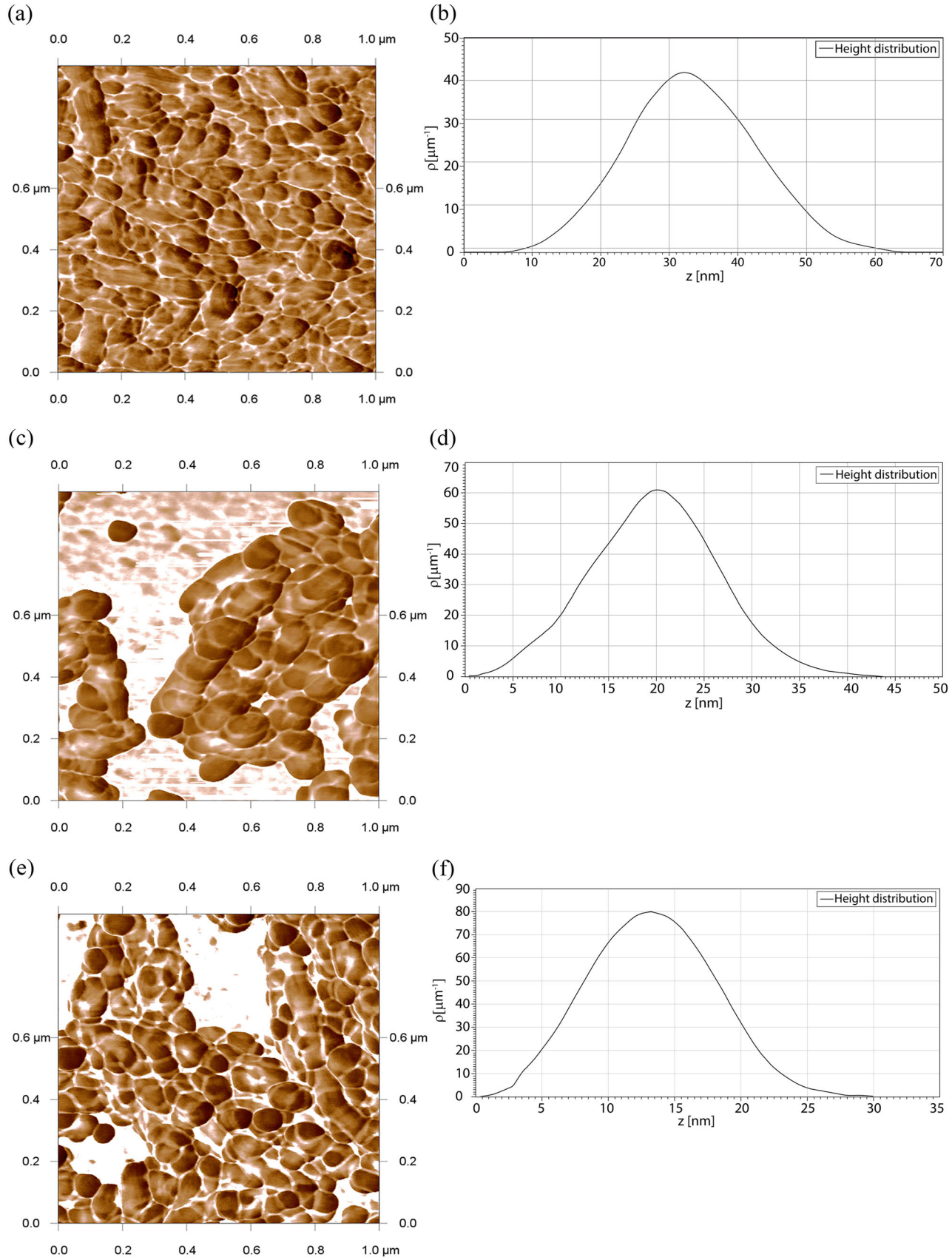

Fig. 1 AFM images of (**a**) BCNC-12, (**c**) BCNC-24 and (**e**) BCNC-72; height distribution of (**b**) BCNC-12, (**d**) BCNC-24 and (**f**) BCNC-72

Table 1 Diameter and Crystallinity Index (CrI) (mean value ± standard deviation) of BC, BCNC-12, BCNC-24, BCNC-72

Sample	Diameter (nm)	CrI (%)
BC	-	71.24 ± 0.75
BCNC-12	34.5 ± 11.5	87.33 ± 0.94
BCNC-24	23 ± 6.57	87.68 ± 1.13
BCNC-72	16 ± 5.25	87.60 ± 0.79

10–50°, at a scanning speed of 5 °/min. The crystallinity index (CrI) of BCNC was estimated by the intensity of the 200 peak (I_{200}, 2θ = 22.6°) and the lowest peak between the peaks at 200 and 110 (I_{am}, 2θ = 18°) using the Segal method and the equation below (Eq. (1)) [33]:

$$\mathrm{CrI}\% = \frac{(I_{200} - I_{am})}{I_{200}} \mathrm{x}\ 100 \quad (1)$$

where I_{200} represents both a crystalline and an amorphous material and I_{am} represents an amorphous material. For PVA/BCNC composites, the samples were prepared in a rectangular shape and scanned over the same range of 2θ.

Thermogravimetric analysis (TGA)

The thermal properties of the BCNC and PVA/BCNC composites were determined using a thermogravimetric analyzer (Mettler Toledo, Model TGA/SDTA 851^e, Switzerland) for TGA and derivative thermogravimetric analysis (dTG). The samples were heated from 50 °C to 600 °C with a scanning rate of 10 °C min^{-1} under a nitrogen atmosphere. The weight of each sample was in the range 2–5 mg.

Opacity and thickness of composite film

The sample thickness was measured by Electronic Digital Caliper (Keiba, 111-101HB 6″, Japan). The thickness of film was randomly recorded at least five positions on the films and an average value of five repeats represented each film composite. The opacity index was carried out using a Genesys 10S UV-Vis spectrophotometer (Thermo Fisher Scientific, USA). The films (0.5 × 5 cm) were placed in a spectrophotometer test cell. The opacity index was calculated by Eq. (2).

$$\text{Opacity index} = \frac{\mathrm{Ab}_{600}}{\text{Film thickness}} \quad (2)$$

where Ab_{600} was the value of absorbance at 600 nm and the film thickness of film was measured in mm [34].

Mechanical properties of composite film

The films were cut into 1.5 cm wide × 15 cm long strips and were kept in a desiccator with $Mg(NO_3)_2$ at 23 °C and a relative humidity of 50% for 48 h. A Universal Testing Machine (Shimadzu model AGS5kN, Japan) was used to analysis tensile test in accordance with ASTM D882–12 (2012). The samples were tested at ambient temperature and an average value of five repeats represented each treatment.

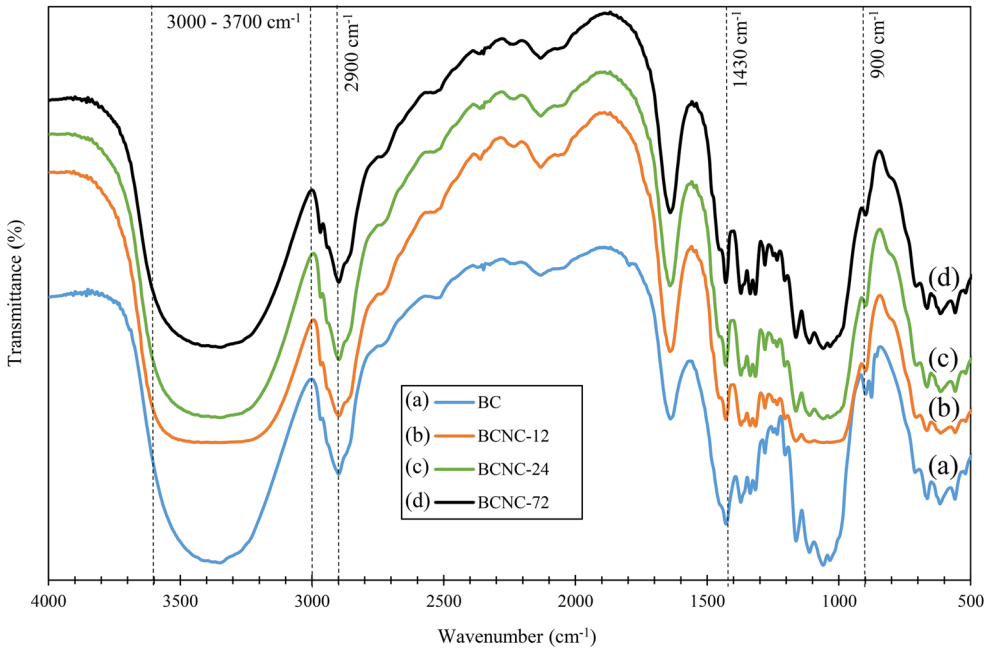

Fig. 2 FTIR spectra of (*a*) BC, (*b*) BCNC-12, (*c*) BCNC-24 and (*d*) BCNC-72

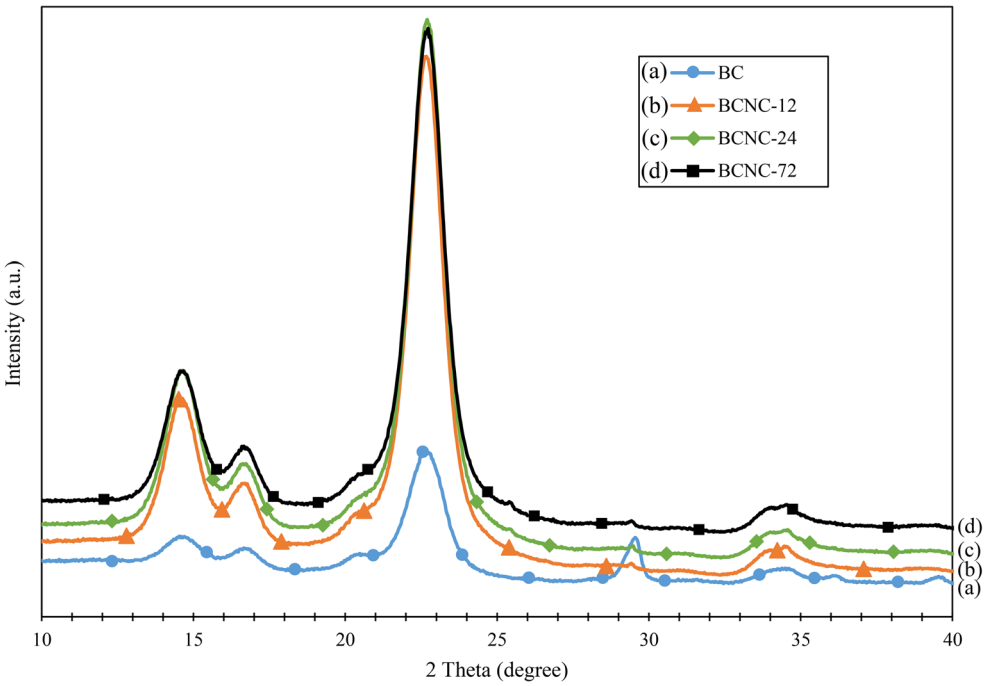

Fig. 3 XRD patterns of (*a*) BC, (*b*) BCNC-12, (*c*) BCNC-24 and (*d*) BCNC-72

Results and discussion

Morphology of BCNC

The morphology of BCNC was investigated using AFM and the diameter of nano particles was estimated using the ImageJ software. Fig. 1 shows a decrease trend in particles diameter as extending of hydrolysis time, which indicated that the obtained BCNC had a spherical shape due to the amorphous regions hydrolysis leading to shorter nanocrystals. The diameter of each BCNC with differing hydrolysis times is shown in Table 1. The diameters of all BCNCs were in the range 16–35 nm, which was also reported by Araki et al. [35]. It is well-document that BC has a higher crystallinity and a smaller amorphous area in its nanofibrils. Therefore, acid hydrolysis amorphous region resulted in the larger diameter of BCNC than that of nanocellulose from plants (5–10 nm) [35]. Moreover, with increasing hydrolysis time, the diameter decreased, indicating that longer hydrolysis treatments led to more digestion of the amorphous region. In this study, a decrease tendency in nanocellulose size with increasing hydrolysis time shared the similar result to the previous report of Martínez-Sanz et al. [22]. Furthermore, the diameter of nanocellulose is a crucible factor affecting to its reinforcement and incorporation of the polymeric matrix that was found in study of Eichhorn et al. [23].

Fourier transform infrared (FTIR) spectroscopy analysis of BCNC

The chemical structures of bacterial cellulose and nanocellulose were investigated using FTIR to confirm the effect of sulfuric acid hydrolysis on the physical structure of the cellulose alone. The FTIR spectra of BC and BCNC at different hydrolysis times are shown in Fig. 2. The bands at 3000–3700 cm^{-1}, 2900 cm^{-1}, 1430 cm^{-1} and 900 cm^{-1} are representative of the cellulose molecular order, corresponding to O–H stretching intramolecular hydrogen bonds, −CH- stretching, CH_2 symmetric bending and β-glycosidic linkage, respectively [36]. These bands were representative of molecular cellulose [22]. Clearly, there were no notable differences among BC and BCNC-12, BCNC-24 and BCNC-72 indicating the absence of chemical modification in the cellulose structure.

Table 2 Thermal properties of BC, BCNC-12, BCNC-24, BCNC-72

Samples	T_{onset} (°C)	Weight loss (%)	T_{max} (°C)	Weight loss (%)	Residue at 600 °C (%)
BC	268.5	7.32	355.3	60.42	5.78
BCNC-12	190.3	3.45	301.8	38.24	23.51
BCNC-24	181	3.34	294.2	33.68	26.17
BCNC-72	176	3.22	275.8	27.77	24.59

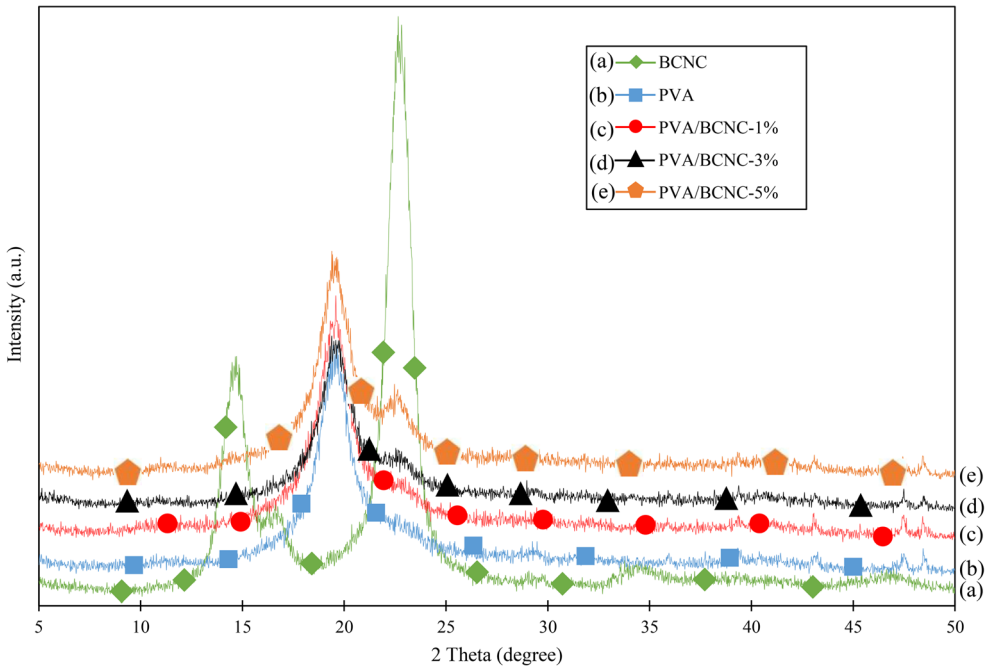

Fig. 4 XRD patterns of (*a*) BCNC, (*b*) PVA, (*c*) PVA/BCNC-1%, (*d*) PVA/BCNC-3% and (*e*) PVA/BCNC-5%

X-ray diffraction (XRD) analysis

The crystallinity of bacterial cellulose and BCNC was investigated using XRD, as shown in Fig. 3. Three major peaks at 14.5°, 16.4° and 22.5° were described as crystalline peaks of BC and the obtained BCNC. The crystallinity index of the obtained BC (71.24%) was similar to that reported for BC (79.06%) in a previous study [22]. The crystallinity of the obtained BCNC-12 increased up to 87.33% after hydrolysis for 12 h. This indicated that sulfuric acid hydrolysis caused a preferential degradation of amorphous regions in the material structure, whereas crystalline regions were domains with higher resistant ability to acid [37]. The higher crystallinity of BCNC compared with that of BC was found in research of Martínez-Sanz et al. [22]. Hence, sulfuric acid hydrolysis treatment can increase the crystallinity of BC by removal of disordered structure.

Thus, the crystallinity of BCNC increased up to 87% considering all the various hydrolysis times. It has been reported that the highest crystallinity of BCNC resulted from hydrolysis for 48 h (90.31%) [22]. This was similar to the crystallinity obtained with BCNC-24 in this study (87.68%). When compared with plant cellulose, Johar et al. [38] reported that the crystallinity of cellulose nanocrystals increased to 59% from that in untreated rice husk (46.8%). Thus it could be

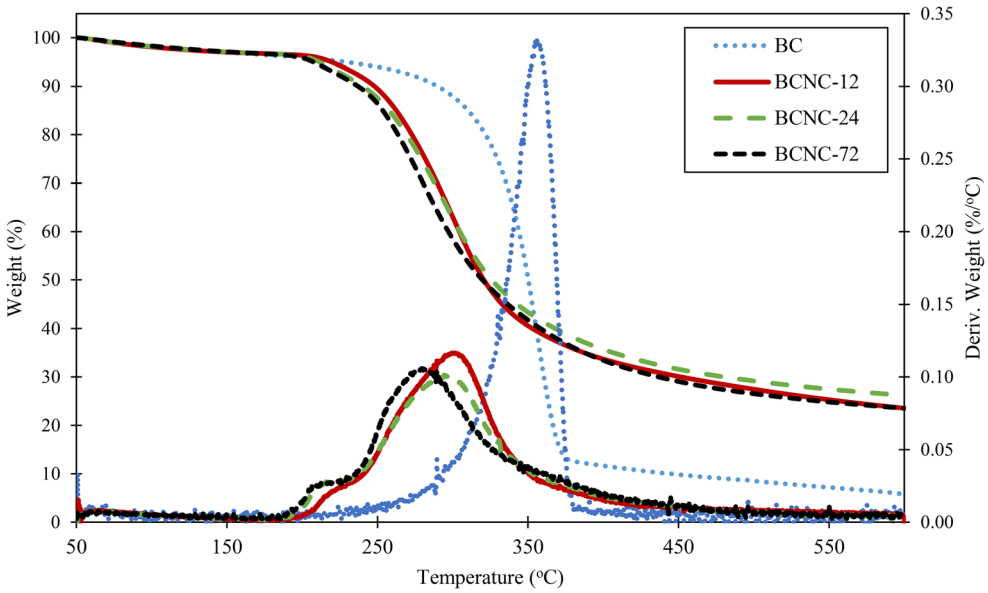

Fig. 5 TG and dTG curves of BC, BCNC-12, BCNC-24 and BCNC-72

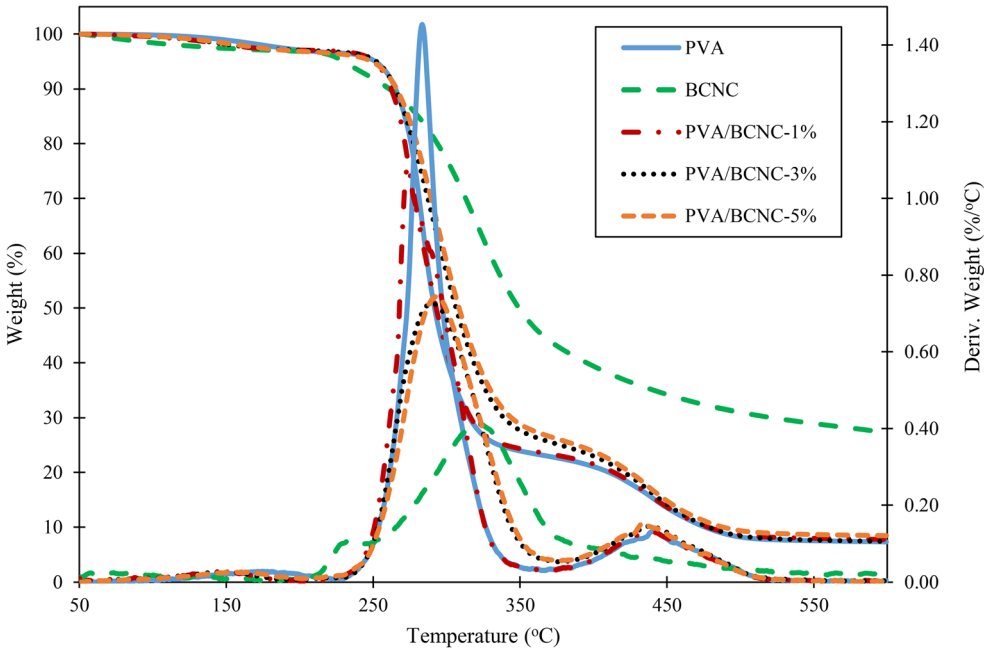

Fig. 6 TG and dTG curves of PVA, BCNC, PVA/BCNC-1%, PVA/BCNC-3% and PVA/BCNC-5%

concluded that BCNC has higher crystallinity than did the nanocellulose from plants, due to the higher purity of the BC structure, whereas plant cellulose is more likely to be associated with hemicellulose and lignin, corresponding to amorphous domains [9, 39]. Thus, BCNC has a higher efficiency for use as a reinforcing agent and in mechanical applications.

On the other hand, the study of the effect of hydrolysis time on the degree of crystallinity based on the crystallinity index shown in Table 2, emphasized no significant differences among BCNC-12, BCNC-24 and BCNC-72. This could have been due to the complete removal of the amorphous region in the cellulose materials during 12 h of hydrolysis and confirmed the high resistance of the crystallinity regions in the BCNC structure to acid hydrolysis. The crystallinity of BCNC after 48 h and 69 h hydrolysis in previous research also showed insignificant differences [22]. Nevertheless, the crystallinity of plant cellulose decreased with increased hydrolysis time from 30 to 40 min in soy hull, due to the destruction of the crystalline structure from within the amorphous region [40]. This implied that BC has a highly crystalline network structure compared with plant cellulose, whereas BC required a long hydrolysis time to break down the fibril bundles to remove the amorphous regions [21]. Therefore, there was no effect on the crystallinity of BCNC with increased hydrolysis time. However, BCNC-24 had the highest crystallinity index and its diameter was about 23 nm and suitable for using for reinforcing PVA composites.

The XRD graphs were used to study the PVA/BCNC composites and are illustrated in Fig. 4. The PVA curve showed a main peak at 2 = 19.5°, corresponding to the semicrystalline domains of PVA [41]. BCNC was detected in the composite

Table 3 The thickness and opacity value (mean value ± standard deviation) of PVA, PVA/BCNC films

Sample	Thickness (mm)	Opacity
PVA	0.22 ± 0.01	0.19 ± 0.01
PVA/BCNC-1%	0.24 ± 0.05	0.25 ± 0.01
PVA/BCNC-3%	0.25 ± 0.11	0.27 ± 0.04
PVA/BCNC-5%	0.18 ± 0.02	0.48 ± 0.04

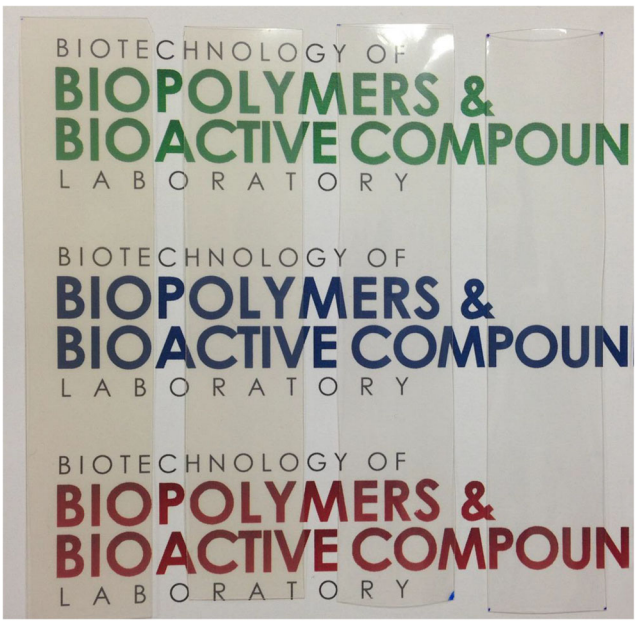

Fig. 7 Visual observation of PVA/BCNC films

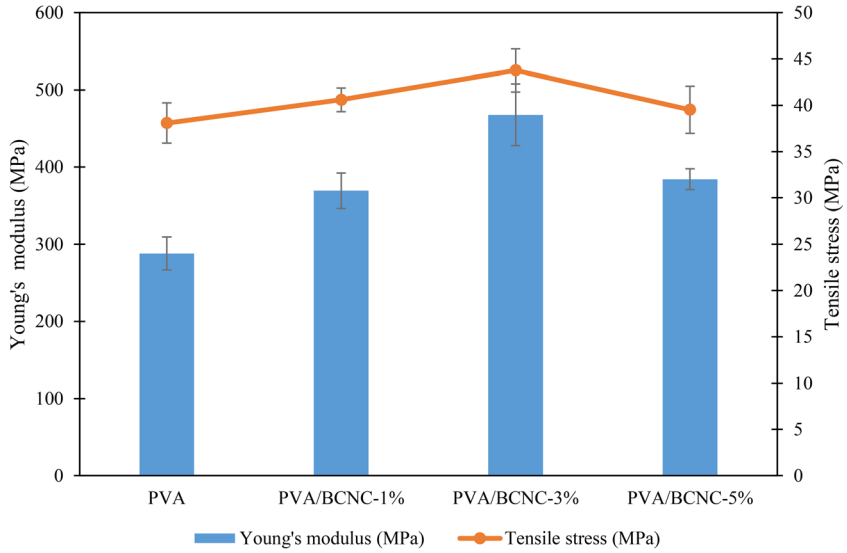

Fig. 8 Mechanical behaviors of PVA/BCNC composites

by the presence of a peak at 2theta = 22.5°, corresponding to the crystalline regions of BCNC [42]. As can be seen, the higher concentration of BCNC led to an increase in the intensity of the 22.5° peak. Specifically, PVA/BCNC-5% had the highest intensity at 2 = 22.5°. As a result, the crystalline percentage of PVA/BCNC was recorded higher due to the present of a crystalline component.

Thermal analysis

Thermogravimetric analyses (TGA) revealed the effect of hydrolysis time on the thermal stability of the obtained nanocellulose. Fig. 5 shows the TG and dTG curves of BC and the nanocellulose obtained after different hydrolysis times. The onset temperature defines the first degradation step of cellulose materials, corresponding to the degradation stages of cellulose such as the depolymerisation, dehydration and decomposition of glycosyl units [35]. There was a lower degradation temperature of the BCNC after sulfuric acid hydrolysis.

As shown in Table 2, the onset temperature of BC was 268.5 °C, and the nanocellulose obtained after 12 h hydrolysis had lower thermal stability at 190.3 °C due to the breakdown of hydrogen bonds between cellulose chains, which were replaced by sulfate groups, resulting in lower thermal stability [43]. As a result, the thermal stability of the obtained BCNC decreased when longer hydrolysis treatment was applied to below 200 °C, due to the increasing of sulfate groups in BCNC. The decrease of thermal stability in BCNC compared to BC was recorded and the explanation for this could be the pyrolysis of the regions with full of sulfate [44]. A similar phenomenon was found in cellulose nanocrystals isolated from plant cellulose [40].

The thermal stability of PVA/BCNC was investigated by the TGA and dTG graphs. Fig. 6 shows the TGA curves for all samples. Water evaporation was responsible for the initial weight loss in all samples at about 70–100 °C [31]. The main degradation peak for all films was recorded around 250–300 °C (Fig. 6). The neat PVA was hydrolyzed at a lower temperature (285 °C) than for the composites, which was 290 and 295 °C for 3 and 5 wt% of BCNC concentrations, respectively. The improvement in the thermal properties of PVA/BCNC at 3 and 5 wt.% could be attributed to the BCNC component which was known as a higher thermally resistant agent in the composites. However, the lower thermal stability of PVA/BCNC-1% (275 °C) than that of the neat PVA could be due to the large contacted surface area of spherical BCNC at low concentration [45]. The similar result was reported by Lu et al. [46] and Ten et al. [47] because of thermal conductivity of the added nanocellulose.

The dTG graphs (Fig. 6) show a shoulder presenting at around 440 °C in all samples, due to polyene chains hydrolyzing to carbon [48]. Clearly, the reinforcing effect of BCNC was exhibited in the enhancement of thermal behavior.

Opacity and visual examination of the PVA/BCNC composite

The opacity index and visual observation of the composites are shown in Table 3 and Fig. 7, respectively. This optical property was related to the incorporation of BCNC and PVA and the concentration of BCNC in the matrix. The opacity values of PVA/BCNC composites had an increase trend, corresponding to the increase of BCNC content. In detail, the opacity of the neat PVA film was recorded at 0.19 ± 0.01 while that of PVA/BCNC-5% peaked at 0.48 ± 0.04. The higher opacity value related to the lower transmittance due to the higher density of solid ingredients in the matrix. On the other hand, Fig. 7 shows the transparency of the film with different clear visibility of the letters in the background according to the

concentration of BCNC [49]. Furthermore, no agglomeration of BCNC was seen in any film, confirming the uniform dispersion of BCNC in the PVA matrix [50].

Mechanical behavior of the PVA/BCNC films

Tensile testing of the PVA/BCNC films was undertaken at room temperature. Fig. 8 summarizes the tensile stress and Young's modulus of the composite films at various BCNC concentrations. The tensile stress and modulus both showed increased trends from 0 to 3 wt% of BCNC content and reached maximum MPa values with PVA/BCNC-3%. Specifically, Young's modulus was 60% higher than in neat PVA film while the tensile strength peaked at 43 MPa. These results were due to the reinforcing effect of BCNC on the PVA matrix. However, a continuous increase in the BCNC content led to failure in both Young's modulus and the tensile stress with values of only 384 MPa and 39 MPa, respectively. Clearly, the homogenous dispersion of BCNC into the matrix had a synergistic effect on the improvement of the mechanical properties of PVA/BCNC films. At the highest BCNC content, the composite recorded a reduction in the Young's modulus resulting from an overload of BCNC that in turn resulted in the possible aggregation of reinforcing agents [51].

Conclusions

The effect of the duration of sulfuric acid hydrolysis on the morphology, crystallinity and thermal stability of BC was optimized for BCNC extraction. The obtained BCNC had a spherical shape with decreasing of diameter in extending the hydrolysis time. The crystallinity of the obtained BCNC was increased up to 87.68% after 24 h, in comparison with BC. However, the thermal stability of the BCNC decreased with longer hydrolysis periods and was lower than in BC due to the substitution of sulfate groups on the cellulose surface. Moreover, the reinforcing effect of the BCNC on the PVA matrix was confirmed in terms of mechanical and thermal behavior.

Acknowledgements The authors are grateful to the Department of Biotechnology, Faculty of Agro-Industry, Kasetsart University, Bangkok and to Kasetsart University, Thailand for supplying facilities and to the Scholarship Program for International Graduate Students 2014.

References

1. Klemm D, Heublein B, Fink H-P, Bohn A (2005) Cellulose: fascinating biopolymer and sustainable raw material. Angew Chem Int Ed 44(22):3358–3393. doi:10.1002/anie.200460587
2. Habibi Y, Lucia LA, Rojas OJ (2010) Cellulose nanocrystals: chemistry, self-assembly, and applications. Chem Rev 110(6): 3479–3500. doi:10.1021/cr900339w
3. Chen X, Yu J, Zhang Z, Lu C (2011) Study on structure and thermal stability properties of cellulose fibers from rice straw. Carbohydr Polym 85(1):245–250. doi:10.1016/j.carbpol.2011.02.022
4. Horn SJ, Nguyen QD, Westereng B, Nilsen PJ, Eijsink VGH (2011) Screening of steam explosion conditions for glucose production from non-impregnated wheat straw. Biomass Bioenergy 35(12): 4879–4886. doi:10.1016/j.biombioe.2011.10.013
5. Teixeira EM, Corrêa AC, Manzoli A, Fabio dLL, Cauê Ribeiro dO, Mattoso LHC (2010) Cellulose nanofibers from white and naturally colored cotton fibers. Cellulose 17(3):595–606. doi:10.1007/s10570-010-9403-0
6. Thygesen A, Oddershede J, Lilholt H, Thomsen AB, Stahl K (2005) On the determination of crystallinity and cellulose content in plant fibres. Cellulose 12(6):563–576. doi:10.1007/s10570-005-9001-8
7. Klemm D, Kramer F, Moritz S, Lindstrom T, Ankerfors M, Gray D, Dorris A (2011) Nanocelluloses: a new family of nature-based materials. Angew Chem, Int Ed Engl 50(24):5438–5466. doi:10.1002/anie.201001273
8. Yamanaka S, Watanabe K, Kitamura N, Iguchi M, Mitsuhashi S, Nishi Y, Uryu M (1989) The structure and mechanical properties of sheets prepared from bacterial cellulose. J Mater Sci 24(9):3141–3145. doi:10.1007/bf01139032
9. Iguchi M, Yamanaka S, Budhiono A (2000) Bacterial cellulose—a masterpiece of nature's arts. J Mater Sci 35(2):261–270. doi:10.1023/A:1004775229149
10. Wan Y, Hong L, Jia S, Huang Y, Zhu Y, Wang Y, Jiang H (2006) Synthesis and characterization of hydroxyapatite–bacterial cellulose nanocomposites. Compos Sci Technol 66(11–12):1825–1832. doi:10.1016/j.compscitech.2005.11.027
11. Ha EYW, Landi CD (1998) Steam explosion treatment of cellulose source, extraction to remove hemicellulose and lignin. US5769934 A
12. Gindl W, Keckes J (2004) Tensile properties of cellulose acetate butyrate composites reinforced with bacterial cellulose. Compos Sci Technol 64(15):2407–2413. doi:10.1016/j.compscitech.2004.05.001
13. Millon LE, Wan WK (2006) The polyvinyl alcohol–bacterial cellulose system as a new nanocomposite for biomedical applications. J Biomed Mater Res, Part B 79B(2):245–253. doi:10.1002/jbm.b.30535
14. Park W-I, Kang M, Kim H-S, Jin H-J (2007) Electrospinning of poly(ethylene oxide) with bacterial cellulose whiskers. Macromol Symp 249-250(1):289–294. doi:10.1002/masy.200750347
15. Svensson A, Nicklasson E, Harrah T, Panilaitis B, Kaplan DL, Brittberg M, Gatenholm P (2005) Bacterial cellulose as a potential scaffold for tissue engineering of cartilage. Biomaterials 26(4):419–431. doi:10.1016/j.biomaterials.2004.02.049
16. Moon RJ, Martini A, Nairn J, Simonsen J, Youngblood J (2011) Cellulose nanomaterials review: structure, properties and nanocomposites. Chem Soc Rev 40:3941–3994. doi:10.1039/c0cs00108b
17. Ranby BG (1949) Aqueous colloidal solutions of cellulose micelles. Acta Chem Scand 3:649–650
18. Lu P, Hsieh Y-L (2010) Preparation and properties of cellulose nanocrystals: rods, spheres, and network. Carbohydr Polym 82(2): 329–336. doi:10.1016/j.carbpol.2010.04.073
19. Wang N, Ding E, Cheng R (2007) Thermal degradation behaviors of spherical cellulose nanocrystals with sulfate groups. Polymer 48(12):3486–3493. doi:10.1016/j.polymer.2007.03.062
20. Wang N, Ding E, Cheng R (2008) Preparation and liquid crystalline properties of spherical cellulose nanocrystals. Langmuir 24(1):5–8. doi:10.1021/la702923w

21. Olsson RT, Kraemer R, López-Rubio A, Torres-Giner S, Ocio MJ, JMa L (2010) Extraction of microfibrils from bacterial cellulose networks for electrospinning of anisotropic biohybrid fiber yarns. Macromolecules 43(9):4201–4209. doi:10.1021/ma100217q
22. Martínez-Sanz M, Lopez-Rubio A, Lagaron JM (2011) Optimization of the nanofabrication by acid hydrolysis of bacterial cellulose nanowhiskers. Carbohydr Polym 85(1):228–236. doi:10.1016/j.carbpol.2011.02.021
23. Eichhorn SJ, Dufresne A, Aranguren M, Marcovich NE, Capadona JR, Rowan SJ, Weder C, Thielemans W, Roman M, Renneckar S, Gindl W, Veigel S, Keckes J, Yano H, Abe K, Nogi M, Nakagaito AN, Mangalam A, Simonsen J, Benight AS, Bismarck A, Berglund LA, Peijs T (2010) Review: current international research into cellulose nanofibres and nanocomposites. J Mater Sci 45(1):1–33. doi:10.1007/s10853-009-3874-0
24. Hamad W (2006) On the development and applications of cellulosic nanofibrillar and nanocrystalline materials. Can J Chem Eng 84(5):513–519. doi:10.1002/cjce.5450840501
25. Siqueira G, Bras J, Dufresne A (2010) Cellulosic bionanocomposites: a review of preparation, properties and applications. Polymers 2(4):728–765. doi:10.3390/polym2040728
26. Visakh PM, Thomas S (2010) Preparation of bionanomaterials and their polymer nanocomposites from waste and biomass. Waste Biomass Valori 1(1):121–134. doi:10.1007/s12649-010-9009-7
27. Favier V, Canova GR, Cavaillé JY, Chanzy H, Dufresne A, Gauthier C (1995) Nanocomposite materials from latex and cellulose whiskers. Polym Adv Technol 6(5):351–355. doi:10.1002/pat.1995.220060514
28. Kvien I, Sugiyama J, Votrubec M, Oksman K (2007) Characterization of starch based nanocomposites. J Mater Sci 42(19):8163–8171. doi:10.1007/s10853-007-1699-2
29. Peresin MS, Habibi Y, Zoppe JO, Pawlak JJ, Rojas OJ (2010) Nanofiber composites of polyvinyl alcohol and cellulose nanocrystals: manufacture and characterization. Biomacromolecules 11(3):674–681. doi:10.1021/bm901254n
30. Xu X, Yang YQ, Xing YY, Yang JF, Wang SF (2013) Properties of novel polyvinyl alcohol/cellulose nanocrystals/silver nanoparticles blend membranes. Carbohydr Polym 98(2):1573–1577. doi:10.1016/j.carbpol.2013.07.065
31. Voronova MI, Surov OV, Guseinov SS, Barannikov VP, Zakharov AG (2015) Thermal stability of polyvinyl alcohol/nanocrystalline cellulose composites. Carbohydr Polym 130:440–447. doi:10.1016/j.carbpol.2015.05.032
32. Duman O, Tunç S, Çetinkaya A (2012) Electrokinetic and rheological properties of kaolinite in poly(diallyldimethylammonium chloride), poly(sodium 4-styrene sulfonate) and poly(vinyl alcohol) solutions. Colloid Surf A 394:23–32. doi:10.1016/j.colsurfa.2011.11.018
33. Segal L, Creely J, Martin AJ, Conrad C (1962) An empirical method for estimating the degree of crystallinity of native cellulose using the x-ray diffractometer. Text Res J 29:786–794
34. Tunç S, Duman O (2011) Preparation of active antimicrobial methyl cellulose/carvacrol/montmorillonite nanocomposite films and investigation of carvacrol release. LWT Food Sci Technol 44(2):465–472. doi:10.1016/j.lwt.2010.08.018
35. Araki J, Wada M, Kuga S (2001) Steric stabilization of a cellulose microcrystal suspension by poly(ethylene glycol) grafting. Langmuir 17(1):21–27. doi:10.1021/la001070m
36. Mandal A, Chakrabarty D (2011) Isolation of nanocellulose from waste sugarcane bagasse (SCB) and its characterization. Carbohydr Polym 86(3):1291–1299. doi:10.1016/j.carbpol.2011.06.030
37. De Souza Lima MM, Wong JT, Paillet M, Borsali R, Pecora R (2003) Translational and rotational dynamics of rodlike cellulose whiskers. Langmuir 19(1):24–29. doi:10.1021/la020475z
38. Johar N, Ahmad I, Dufresne A (2012) Extraction, preparation and characterization of cellulose fibres and nanocrystals from rice husk. Ind Crop Prod 37(1):93–99. doi:10.1016/j.indcrop.2011.12.016
39. Wan YZ, Luo H, He F, Liang H, Huang Y, Li XL (2009) Mechanical, moisture absorption, and biodegradation behaviours of bacterial cellulose fibre-reinforced starch biocomposites. Compos Sci Technol 69(7–8):1212–1217. doi:10.1016/j.compscitech.2009.02.024
40. Neto WPF, Silvério HA, Dantas NO, Pasquini D (2013) Extraction and characterization of cellulose nanocrystals from agro-industrial residue – soy hulls. Ind Crop Prod 42:480–488. doi:10.1016/j.indcrop.2012.06.041
41. Sriupayo J, Supaphol P, Blackwell J, Rujiravanit R (2005) Preparation and characterization of α-chitin whisker-reinforced poly(vinyl alcohol) nanocomposite films with or without heat treatment. Polymer 46(15):5637–5644. doi:10.1016/j.polymer.2005.04.069
42. Moharram MA, Mahmoud OM (2007) X-ray diffraction methods in the study of the effect of microwave heating on the transformation of cellulose I into cellulose II during mercerization. J Appl Polym Sci 105(5):2978–2983. doi:10.1002/app.26580
43. Roman M, Winter WT (2004) Effect of sulfate groups from sulfuric acid hydrolysis on the thermal degradation behavior of bacterial cellulose. Biomacromolecules 5(5):1671–1677. doi:10.1021/bm034519+
44. Martinez-Sanz M, Lopez-Rubio A, Lagaron JM (2013) High-barrier coated bacterial cellulose nanowhiskers films with reduced moisture sensitivity. Carbohydr Polym 98(1):1072–1082. doi:10.1016/j.carbpol.2013.07.020
45. Pääkkö M, Ankerfors M, Kosonen H, Nykänen A, Ahola S, Österberg M, Ruokolainen J, Laine J, Larsson PT, Ikkala O, Lindström T (2007) Enzymatic hydrolysis combined with mechanical shearing and high-pressure homogenization for nanoscale cellulose fibrils and strong gels. Biomacromolecules 8(6):1934–1941. doi:10.1021/bm061215p
46. Lu J, Askeland P, Drzal LT (2008) Surface modification of microfibrillated cellulose for epoxy composite applications. Polymer 49(5):1285–1296. doi:10.1016/j.polymer.2008.01.028
47. Ten E, Turtle J, Bahr D, Jiang L, Wolcott M (2010) Thermal and mechanical properties of poly(3-hydroxybutyrate-co-3-hydroxyvalerate)/cellulose nanowhiskers composites. Polymer 51(12):2652–2660. doi:10.1016/j.polymer.2010.04.007
48. Lu J, Wang T, Drzal LT (2008) Preparation and properties of microfibrillated cellulose polyvinyl alcohol composite materials. Compos Part A 39(5):738–746. doi:10.1016/j.compositesa.2008.02.003
49. Li W, Yue J, Liu S (2012) Preparation of nanocrystalline cellulose via ultrasound and its reinforcement capability for poly(vinyl alcohol) composites. Ultrason Sonochem 19(3):479–485. doi:10.1016/j.ultsonch.2011.11.007
50. Fortunati E, Luzi F, Puglia D, Terenzi A, Vercellino M, Visai L, Santulli C, Torre L, Kenny JM (2013) Ternary PVA nanocomposites containing cellulose nanocrystals from different sources and silver particles: part II. Carbohydr Polym 97(2):837–848. doi:10.1016/j.carbpol.2013.05.015
51. Cho M-J, Park B-D (2011) Tensile and thermal properties of nanocellulose-reinforced poly(vinyl alcohol) nanocomposites. J Ind Eng Chem 17(1):36–40. doi:10.1016/j.jiec.2010.10.006